microorganisms

MDPI

Article

Transcriptome Analysis of Citrus Dwarfing Viroid Induced Dwarfing Phenotype of Sweet Orange on Trifoliate Orange Rootstock

Irene Lavagi-Craddock [1,†], Tyler Dang [1,†], Stacey Comstock [1], Fatima Osman [2], Sohrab Bodaghi [1] and Georgios Vidalakis [1,*]

[1] Department of Microbiology and Plant Pathology, University of California, Riverside, CA 92521, USA; irenela@ucr.edu (I.L.-C.); tdang004@ucr.edu (T.D.); scoms002@ucr.edu (S.C.); sohrab@ucr.edu (S.B.)
[2] Department of Plant Pathology, University of California, Davis, CA 95616, USA; fmosman@ucdavis.edu
* Correspondence: georgios.vidalakis@ucr.edu
† These authors contributed equally to this work.

Abstract: Dwarfed citrus trees for high-density plantings or mechanized production systems will be key for future sustainable citrus production. Citrus trees consist of two different species of scion and rootstock. Therefore, any observed phenotype results from gene expression in both species. Dwarfed sweet orange trees on trifoliate rootstock have been produced using citrus dwarfing viroid (CDVd). We performed RNA-seq transcriptome analysis of CDVd-infected stems and roots and compared them to non-infected controls. The identified differentially expressed genes validated with RT-qPCR corresponded to various physiological and developmental processes that could be associated with the dwarfing phenotype. For example, the transcription factors MYB13 and MADS-box, which regulate meristem functions and activate stress responses, were upregulated in the stems. Conversely, a calcium-dependent lipid-binding protein that regulates membrane transporters was downregulated in the roots. Most transcriptome reprogramming occurred in the scion rather than in the rootstock; this agrees with previous observations of CDVd affecting the growth of sweet orange stems while not affecting the trifoliate rootstock. Furthermore, the lack of alterations in the pathogen defense transcriptome supports the term "Transmissible small nuclear ribonucleic acid," which describes CDVd as a modifying agent of tree performance with desirable agronomic traits rather than a disease-causing pathogen.

Keywords: RNA-seq; CDVd; transmissible small nuclear ribonucleic acid (TsnRNA); mRNA; functional analysis; differentially expressed genes (DEGs)

Citation: Lavagi-Craddock, I.; Dang, T.; Comstock, S.; Osman, F.; Bodaghi, S.; Vidalakis, G. Transcriptome Analysis of Citrus Dwarfing Viroid Induced Dwarfing Phenotype of Sweet Orange on Trifoliate Orange Rootstock. *Microorganisms* **2022**, *10*, 1144. https://doi.org/10.3390/microorganisms10061144

Academic Editors: Nuria Duran-Vila and Pedro Serra Alfonso

Received: 30 March 2022
Accepted: 30 May 2022
Published: 1 June 2022

1. Introduction

Citrus (family *Rutaceae*) is an economically important crop with several high-value cultivars, including oranges, mandarins, grapefruits, and lemons. The citrus industry was recently valued at USD3.63 billion in California alone, with an estimated economic impact of USD7.6 billion [1]. Citrus fruits and flavors have a wide range of usage and are important sources of vitamins, antioxidants, minerals, and dietary fiber essential for overall nutritional wellbeing [2,3]. Citrus trees are produced by grafting the desired scion variety onto a suitable rootstock species and then planting it in commercial citrus orchards. Tree spacing in citrus orchards has reduced over time in favor of higher tree densities to maintain yield on the reduced available land for agriculture, increase economic returns, and combat the growing threat of citrus huanglongbing (HLB). However, high-density citrus plantings cannot be achieved without the use of dwarfed citrus trees [4–7].

Viroid infection can induce morphological and cytological changes that have been well documented for other plant and viroid species [8–10]. Viroid symptoms can include leaf epinasty, chlorosis, stunting, and reduced root mass. Other symptoms such as distorted cell

walls, plasma membrane, mitochondria, and chloroplasts have also been observed [11–13]. In contrast, the citrus dwarfing viroid (CDVd) does not appear to cause major growth abnormalities and has been studied as a graft-transmissible dwarfing agent [14–19].

In addition, CDVd-induced symptoms on citrus hosts depend on species, variety, and rootstock. CDVd infection of navel orange trees [*Citrus sinensis* (L.) Osbeck] propagated on trifoliate rootstock [*C. trifoliata* (L.), syn. *Poncirus trifoliata* (L.) Raf.] has shown that the observed stunting phenotype induced by CDVd-infection reduces canopy volume by approximately 50% (Figure 1), and the reduction in the canopy volume is a result of a >20% decrease in the apical growth of the shoots [19–21].

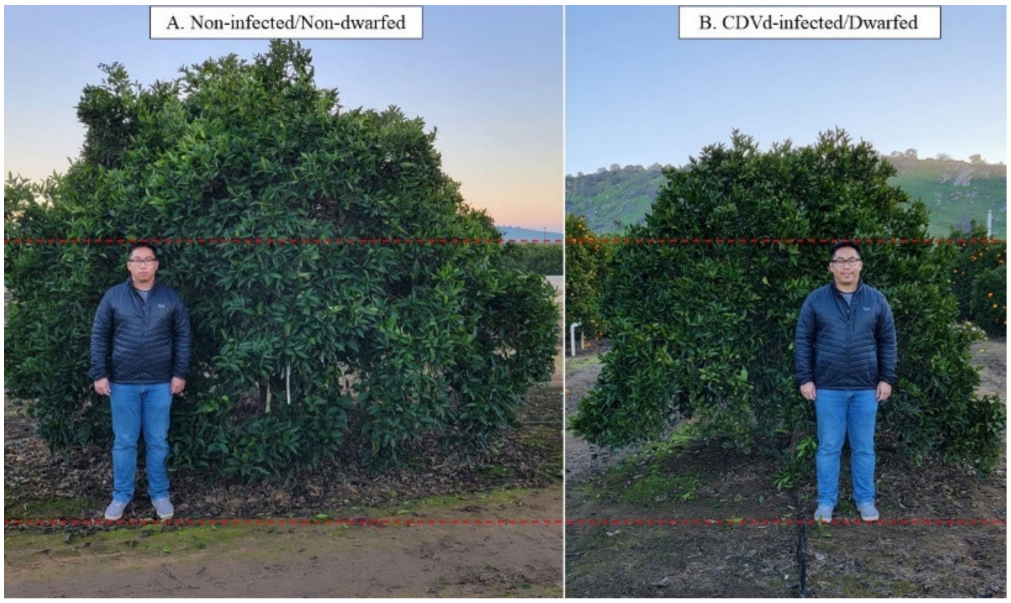

Figure 1. The observed dwarfing phenotype in navel orange (*Citrus sinensis* (L.) Osbeck) on trifoliate (*Citrus trifoliata* (L.) Raf.) rootstock. (**A**) is the non-infected/non-dwarfed tree and (**B**) is the citrus dwarfing viroid (CDVd)-infected/dwarfed tree.

Therefore, there is a need to elucidate the molecular mechanism of the dwarfing phenotype, so the valuable information can be used to produce dwarfed trees for high-density plantings.

Currently, identifying potential targets of CDVd is challenging due to the nature of viroids, which do not encode for proteins, limiting the experimental approaches. In addition, most of the data on symptom induction by single viroids refer to experimental tests on the biological indicator 'Etrog' citron (*C. medica* L.). Previously, studies on CDVd-induced differentially expressed genes were performed on 'Etrog' citron in growth chamber conditions; microarray analysis identified mainly genes related to the cell wall structure, amino acid transport, signal transduction, and plant defense/stress response [22]. To this date, there are no transcriptome studies on mature dwarfed citrus field trees infected with CDVd [9].

To further explore the global effect of CDVd-infection on citrus host mRNAs and gain insight into the symptom development mechanism leading to the dwarfed phenotype observed in field plantings, we performed a transcriptome analysis of CDVd-infected dwarf citrus trees using a high throughput sequencing (HTS) approach. There has been limited transcriptomic research on citrus host response to viroid infection using the bioindicator 'Etrog' citron [23], while other viroid studies have used model plant systems such as *Solanum lycopersicum* and *Nicotiana tabacum* [11,24,25].

The improved availability of citrus genome and annotation has enabled the widespread use of HTS studies to develop a global understanding of the molecular machinery behind the response to pathogen infection [26]. Furthermore, HTS allows the discovery of rare

transcripts, which would be difficult to identify using traditional methods such as microarrays, and is more time efficient than an RT-qPCR approach. More specifically, in citrus, HTS analysis of mRNA has been widely used to understand host responses to pathogens such as '*Candidatus*' Liberibacter asiaticus [27–30] and citrus tristeza virus [28,31].

In this study, we performed a comparative analysis of differentially expressed genes in the stems and roots of CDVd-infected and non-infected sweet orange scion on trifoliate orange rootstock. This analysis provides valuable molecular information to understand the mechanisms responsible for the citrus dwarf phenotype in the field.

2. Materials and Methods

2.1. Plant Materials and RNA Isolation

Plant materials were collected in April 2016 from 18-year-old 'Parent Washington' navel orange on 'Rich 16-6′ trifoliate orange trees. All trees were planted in the same east-west running orchard located at the University of California, Agriculture and Natural Resources, Lindcove Research and Extension Center (LREC) in Exeter, CA, USA. CDVd-infected trees were planted at high density (3 × 6.7 m), whereas non-infected control trees were spaced at standard density (6.1 × 6.7 m).

Stem and root samples were collected from the south side of the dwarfed CDVd-infected (n = 3) and the north and south sides of the full-size non-infected trees (n = 3). This type of sampling was necessary to represent the different sizes of trees (i.e., dwarfed trees 61.2% smaller than full size, [21]) and the different light distribution within their canopies due to the size and east-west orientation of the tree rows, in the transcriptome analysis.

After leaves and petioles were removed, the stems were roughly chopped into approximately 0.5–1 cm pieces, placed into 50 mL conical tubes, and flash-frozen with liquid nitrogen in the field. Feeder roots were sampled approximately 1 m away from the trunk and 20 cm deep, near the irrigation emitters, using a 10 cm diameter corer. The feeder root samples were washed thoroughly with water, gently blotted dry with paper towels, chopped into 0.5–1 cm pieces, placed into 50 mL conical tubes, and flash-frozen with liquid nitrogen in the field. Between each sample collection and processing, cutting tools and working surfaces were sanitized with 10% bleach solution (0.5–1% sodium hypochlorite) and then rinsed with water. New sterile disposable plasticware and razor blades were used to chop each sample. The frozen samples were transported to the Citrus Clonal Protection Program (CCPP), Citrus Diagnostic Therapy and Research Laboratory at the UC Riverside (Riverside, CA, USA) on dry ice and stored at −80 °C for downstream analysis (CDFA permit 3477).

Total RNA was isolated using the TRIzol® reagent (Thermo Fisher Scientific, Waltham, MA, USA). For each sample, 300 mg of frozen tissue were ground in liquid nitrogen with sterilized mortar and pestle. The ground material was transferred to a 5 mL Eppendorf tube, and 3 mL of TRIzol® reagent was added immediately. RNA extraction was performed according to the manufacturer's instructions. The eluted RNA was aliquoted into four 1.5 mL microcentrifuge tubes to prevent freezing-thawing cycles during downstream analysis. The RNA concentration and quality were assessed with a spectrophotometer and the Agilent 2100 Bioanalyzer (Agilent, Santa Clara, CA, USA) using the Plant RNA Nano assay. The presence or absence of CDVd, as well as that of other graft-transmissible pathogens of citrus endemic to California, was confirmed in each sample by reverse transcription-quantitative polymerase chain reaction (RT-qPCR) as previously described [21,32].

2.2. Library Preparation and High Throughput Sequencing

Eighteen cDNA libraries were prepared for each sample using the Illumina TruSeq Stranded mRNA Kit (San Diego, CA, USA), following the manufacturer's recommended protocol for Low Sample (LS) throughput. The libraries were quantified with the Agilent 2100 Bioanalyzer (Agilent, Santa Clara, CA, USA) using the High Sensitivity DNA Kit. The libraries were quantified using the in-house SeqMatic HT1 quantitative polymerase chain reaction (qPCR) assay (SeqMatic, Fremont, CA, USA) and pooled equimolar. The libraries

were sequenced using an Illumina HiSeq™ 4000 (San Diego, CA, USA) instrument with paired-end 100 bp reads (SeqMatic, Fremont, CA, USA). Raw reads were trimmed and demultiplexed for subsequent bioinformatic analysis.

2.3. Bioinformatic Analysis

The raw sequencing data of the north and south samples from each of the three non-infected full-size trees were concatenated into one file for analysis. Bioinformatic analyses were performed using the OmicsBox software suite version 2.0.36 (Cambridge, MA, USA) using the reference Valencia orange (version 1.0) (GCF_000317415.1) and trifoliate (v. 1.3.1) [33] genomes. RNA-seq alignment was performed using Spliced Transcript Alignment to a Reference (STAR v. 2.7.8a) [34] with default parameters. The quantification of transcript expression levels was performed using the HTSeq (v. 0.90) package [35], while the differential expression analysis was performed edgeR (v. 3.28.0) [36] with default parameters. Functional analysis was performed using the Blast2GO [37] tool within OmicsBox Suite. BLAST [38] was performed on the DEG sequences, and the gene ontology (GO) terms and Kyoto Encyclopedia of Genes and Genomes (KEGG) functions [39] were assigned. Protein functionality was confirmed with InterPro [40]. The dataset was uploaded into NCBI Sequence Read Archive under the accession numbers SAMN26677719 to SAMN26677722. All figures were created using GraphPad Prism version 9.3.0 (San Diego, CA, USA).

2.4. Expression Analysis of Citrus mRNA Target Genes Using RT-qPCR

RT-qPCR assays were designed to verify the expression levels of the predicted target genes (Supplementary Table S1). Actin was used as an internal control gene to determine the relative abundance of the target mRNA expression levels by the comparative Cq method. Reverse transcription was performed using the SuperScript™ II Reverse Transcriptase (RT) (Thermo Fisher Scientific). The reactions were performed using the manufacturer's recommended protocol as follows: 2 µL of oligo (dT) (500 µg/mL), 2 µL of dNTP (10 mM), 4 µL of total RNA (diluted to 100 µg/µL), and 16 µL of nuclease-free water with a final volume of 24 µL. All samples were standardized to the same concentration to ensure equal representation, and incubation steps were performed using the ProFlex thermal cycler (Thermo Fisher Scientific). The mixture was incubated for 5 min at 65 °C and subsequently chilled on ice. The first strand synthesis was prepared with 8 µL of 5x First-Strand Buffer, 4 µL of 0.1 M DTT, and 2 µL of RNaseOUT™ (40 units/µL) (Thermo Fisher Scientific) and then incubated for 2 min at 42 °C. Finally, 2 µL of SuperScript™ II RT (200 units) were added, and the reaction was incubated at 42 °C for 50 min followed by 15 min at 70 °C. Downstream qPCR was performed in triplicates, according to the MIQE guidelines [41], using the TaqMan™ Fast Advanced Master Mix Kit (Thermo Fisher Scientific) as follows: 10µL of master mix, 8 µL of nuclease-free water, 1 µL of primer and probe mixture, and 1 µL of cDNA. FAM fluorophore was used for all qPCR probes. The qPCR was performed using the QuantStudio 12K Flex Real-Time PCR (Thermo Fisher Scientific) with the following conditions: 50 °C for 2 min, 95 °C for 2 min, and 95 °C for 1 s, 60 °C for 20 s for 40 cycles.

3. Results

3.1. Transcriptome Assembly and Annotation

To understand the citrus host transcriptome response to CDVd infection, we prepared and analyzed RNA-seq libraries from the stem and root samples of non-infected and CDVd-infected navel orange citrus trees on trifoliate orange rootstock. Overall, stems generated more reads than roots for non-infected and CDVd-infected trees (Table 1). A high percentage of reads (72–88%) from both the non-infected and CDVd-infected trees were mapped to their relative genomes using the STAR alignment software (Table 1). The average length of mapped reads in all samples tested was close to the expected size of 200 nt (Table 1).

Table 1. Summary of sequencing and STAR alignment results for non-infected and citrus dwarfing viroid (CDVd)-infected trees from the stem (*Citrus sinensis* (L.) Osbeck) and root tissues (*C. trifoliata* (L.).

Treatment	Avg. Total Reads	Avg. Uniquely Mapped Reads	Avg. Percent Mapped Reads	Avg. Mapped Length
Non-infected stem	57,720,333 ± 7,556,534	40,055,889 ± 10,591,488	71.63%	199.04 ± 0.25
CDVd-infected stem	36,254,830 ± 15,692,505	31,769,508 ± 13,584,944	87.87%	199.51 ± 0.32
Non-infected root	58,030,198 ± 9,821,953	48,928,990 ± 10,744,466	83.95%	199.8 ± 0.2
CDVd-infected roots	25,671,752 ± 1,148,290	22,553,155 ± 1,891,667	87.78%	199.98 ± 0.09

3.2. Differentially Expressed Genes (DEGs) Analysis and Identification

The multidimensional scaling (MDS) plot showed distinct differences between the non-infected and CDVd-infected trees in stem and root tissues (Figure 2A,B). Non-infected stems and roots were similar and clustered closer together than the CDVd-infected tissues (Figure 2A,B).

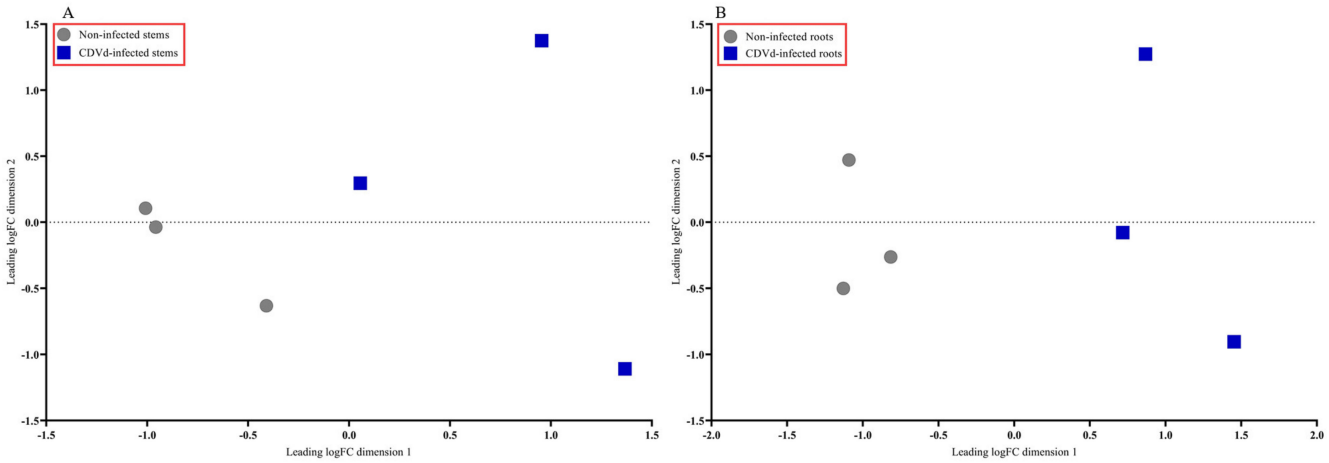

Figure 2. Multidimensional scaling (MDS) plot displaying similarity in leading log fold change in non-infected versus citrus dwarfing viroid (CDVd)-infected (**A**) stem and (**B**) root tissues.

Volcano plots were generated to display the number of up and downregulated DEGs by plotting the log fold change (FC) against the negative log (10)-transformed false discovery rate (FDR) values (Figure 3). Samples with high negative log (10)-transformed FDR values indicate DEGs with more significant regulation in response to CDVd-infection. Positive FC values indicated upregulated DEGs (FDR < 0.05; logFC > 1.0), while negative FC values indicated downregulated ones (FDR < 0.05; logFC < −1.0). Most upregulated DEGs were identified in the stems (83), whereas most of the downregulated DEGs were identified in the roots (186) (Figure 3 and Table 2).

Table 2. Number of upregulated and downregulated differentially expressed genes identified in stem (*Citrus sinensis* (L.) Osbeck) and root tissues (*C. trifoliata* (L.)).

Tissue Type	Upregulated	Downregulated	Total
Stem	83	92	175
Root	48	186	234

Heat maps of the top 50 DEGs identified from the stem and root tissues of non-infected and CDVd-infected trees were generated based on FDR (Figure 4). Results indicated a relatively even clustering of stem upregulated and downregulated DEGs in the non-infected and CDVd-infected samples. In contrast, the roots showed clustering skewed towards the DEGs that were significantly downregulated in the CDVd-infected and upregulated in the non-infected samples (Figure 4A,B).

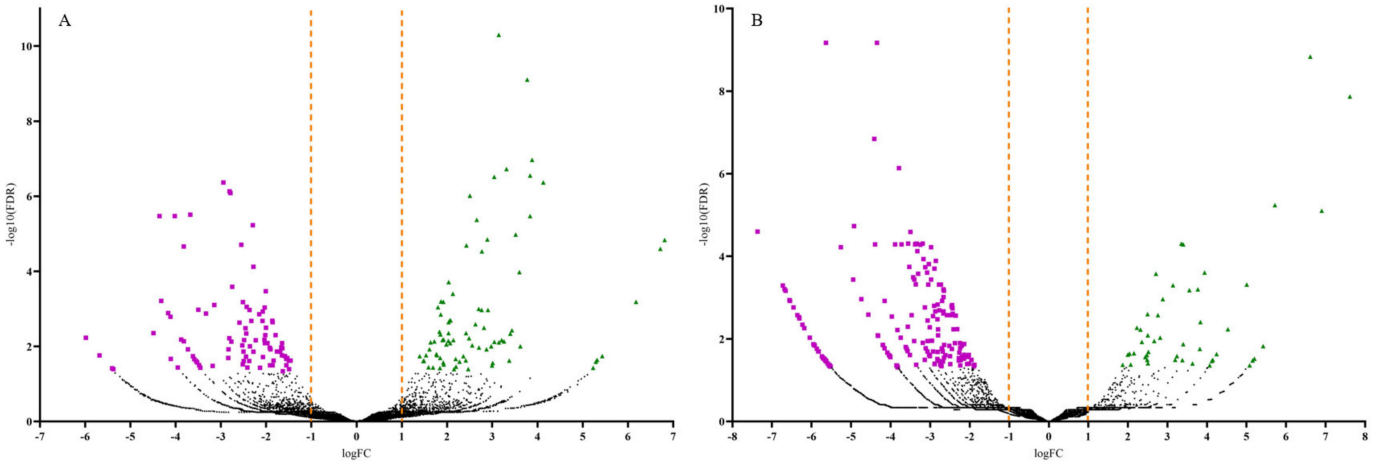

Figure 3. Volcano plots of the differentially expressed genes (DEGs) for both significantly upregulated and downregulated genes between non-infected and citrus dwarfing viroid (CDVd)-infected (**A**) stem and (**B**) root samples. Significantly upregulated (FDR < 0.05; logFC > 1.0) and downregulated (FDR < 0.05; logFC < −1.0) genes are represented in green (triangles) and magenta (squares), respectively.

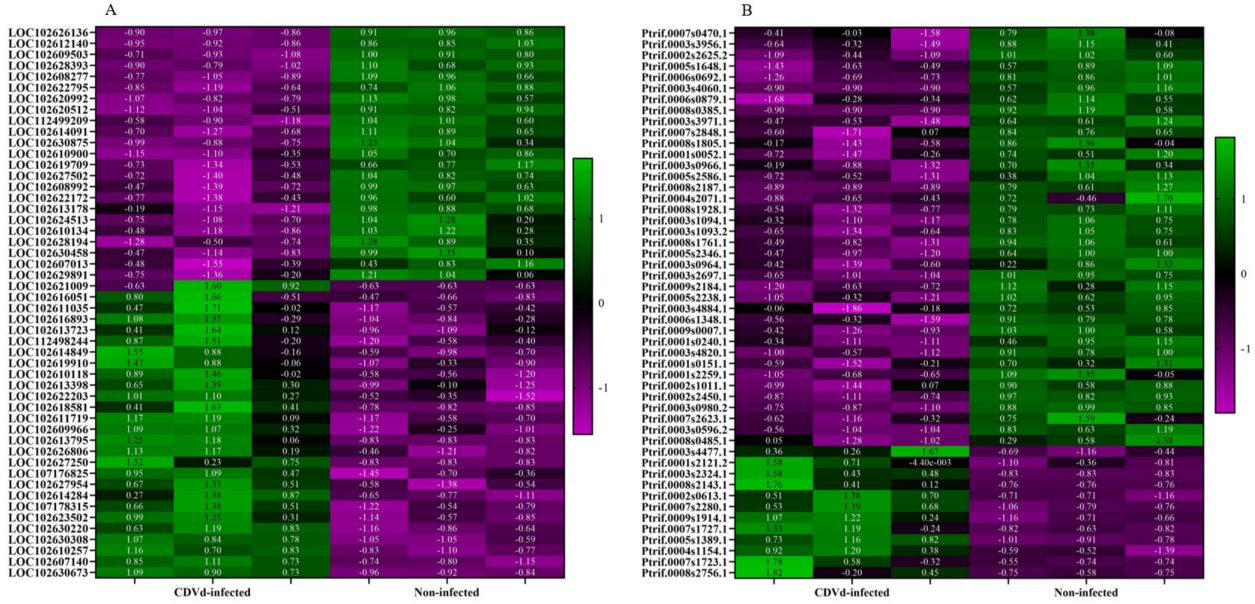

Figure 4. Heat map of the top 50 differentially expressed genes (DEGs) in both (**A**) stems and (**B**) roots ranked by FDR. The targets indicated in green are upregulated DEGs, while magenta targets are downregulated DEGs.

DEG analysis identified up- and downregulated targets. In the stem, the probable 28S rRNA (cytosine-C(5))-methyltransferase (FDR = 5.05×10^{-11}; logFC = 8.83) and the pentatricopeptide repeat-containing protein (FDR = 4.29×10^{-7}; logFC = −2.95) had the most statistically significant fold change (Table 3).

In the roots, the plant invertase/pectin methylesterase inhibitor superfamily protein (FDR = 2.48×10^{-04}; logFC 3.94) and the kinase-inducible domain interacting 9, Kix9 (FDR = 6.75×10^{-10}; logFC = −5.64) had the most statistically significant fold change (Table 4).

Table 3. List of top 5 up and downregulated differentially expressed genes (DEGs) in non-infected vs. citrus dwarfing viroid (CDVd)-infected for stem tissues based on the FDR.

	Accession	Product	Fold Change (FC)	LogFC	Log Count Per Million (CPM)	*p*-Value	FDR
Upregulated stem	LOC102607140	probable 28S rRNA (cytosine-C(5))-methyltransferase	8.83	3.14	11.04	2.70×10^{-15}	5.05×10^{-11}
	LOC102611719	germin-like protein subfamily T member	13.66	3.77	7.41	8.39×10^{-14}	7.84×10^{-10}
	LOC102610118	pentatricopeptide repeat-containing protein At2g17525	14.72	3.88	6.52	1.73×10^{-11}	1.08×10^{-7}
	LOC102616051	cytosolic sulfotransferase 15-like	17.47	4.13	6.04	1.62×10^{-10}	4.29×10^{-7}
	LOC102614284	aspartic proteinase Asp1-like	5.67	2.50	9.39	5.71×10^{-10}	9.70×10^{-7}
Downregulated stem	LOC102627502	pentatricopeptide repeat-containing protein At4g21300	−7.70	−2.95	7.86	1.84×10^{-10}	4.29×10^{-7}
	LOC102620512	SKP1-like protein 21	−7.01	−2.81	8.07	3.56×10^{-10}	7.40×10^{-7}
	LOC102610900	protein SHORT-ROOT-like	−6.90	−2.79	8.06	4.41×10^{-10}	8.24×10^{-7}
	LOC102620992	amino-acid permease BAT1-like	−12.78	−3.68	6.34	1.99×10^{-9}	3.11×10^{-6}
	LOC102628393	serine/threonine-protein kinase ATG1a	−16.21	−4.02	6.03	2.69×10^{-9}	3.38×10^{-6}

Further analysis showed that the highest logFC among the upregulated stem DEGs corresponded to the dihydrolipoyllysine-residue acetyltransferase component 5 of pyruvate dehydrogenase complex, chloroplastic (LOC102627250) (logFC = 6.81; FDR = 1.47×10^{-5}), while the highest logFC for downregulated stem DEGs corresponded to the pentatricopeptide repeat-containing protein, mitochondrial-like (LOC107176200) (logFC = −5.98; FDR 0.005).

The highest logFC for the upregulated root DEGs corresponded to the HSP20-like chaperone super family protein (Ptrif.0003s2324.1) (logFC 7.61; FDR 1.35E−08), and the highest logFC for the downregulated root DEGs corresponded to the calcium-dependent lipid-binding (CaLB domain) family protein (Ptrif.0003s4060.1) (logFC −7.3; FDR 2.53×10^{-5}). The complete list of all DEGs identified in this study can be found in Supplementary Tables S2–S5.

Table 4. List of top 5 up and downregulated differentially expressed genes (DEGs) in non-infected vs. citrus dwarfing viroid (CDVd)-infected for roots tissues based on the FDR.

	Gene ID	Alt Gene ID	Product	Fold Change (FC)	LogFC	Log Count Per Million (CPM)	*p*-Value	FDR
Upregulated roots	Ptrif.0009s1914.1	AT5G62350/LOC_Os06g49760	Plant invertase/pectin methylesterase inhibitor superfamily protein	15.33	3.94	7.00	3.62×10^{-7}	2.48×10^{-4}
	Ptrif.0004s1154.1	AT5G07310/Cre14.g620500/LOC_Os04g32620	Integrase-type DNA-binding superfamily protein	6.54	2.71	12.63	4.04×10^{-7}	2.64×10^{-4}
	Ptrif.0005s1389.1	Cre05.g240400/LOC_Os12g25450	S-adenosyl-L-methionine-dependent O-methyltransferase/ethylene-responsive transcription factor ERF114	8.82	3.14	7.80	1.02×10^{-6}	5.05×10^{-4}
	Ptrif.0005s2465.1	AT5G52010/LOC_Os06g07020	C2H2-like zinc finger protein	7.38	2.88	8.03	2.69×10^{-6}	1.09×10^{-3}
	Ptrif.0006s1595.1	AT5G03800	Pentatricopeptide repeat (PPR) superfamily protein	7.43	2.89	8.06	2.73×10^{-6}	1.09×10^{-3}
Downregulated roots	Ptrif.0001s0240.1	AT4G32295	Kinase-inducible domain interacting 9, Kix9	−49.72	−5.64	9.20	6.04×10^{-14}	6.75×10^{-10}
	Ptrif.0003s0980.2	LOC_Os04g48160	IQ calmodulin-binding motif family protein, putative, expressed	−13.83	−3.79	10.36	1.96×10^{-10}	7.31×10^{-7}
	Ptrif.0006s0692.1	AT2G37740/LOC_Os05g20930	zinc-finger protein 10	−30.39	−4.93	7.76	7.47×10^{-9}	1.85×10^{-05}
	Ptrif.0003s4060.1	AT4G01200	Calcium-dependent lipid-binding (CaLB domain) family protein	−164.81	−7.36	7.11	1.13×10^{-8}	2.53×10^{-5}
	Ptrif.0005s2586.1	AT1G75000/LOC_Os12g43890	GNS1/SUR4 membrane protein family	−11.31	−3.50	9.35	1.27×10^{-8}	2.58×10^{-5}

3.3. Confirmation of Candidate DEGs by RT-qPCR Analysis

To confirm the accuracy of Illumina RNA-seq results, RT-qPCR was performed on selected candidate DEGs. The logFC values of the RNA-seq and RT-qPCR were consistent and showed similar trends for both up- and downregulated stem and root DEGs (Figure 5).

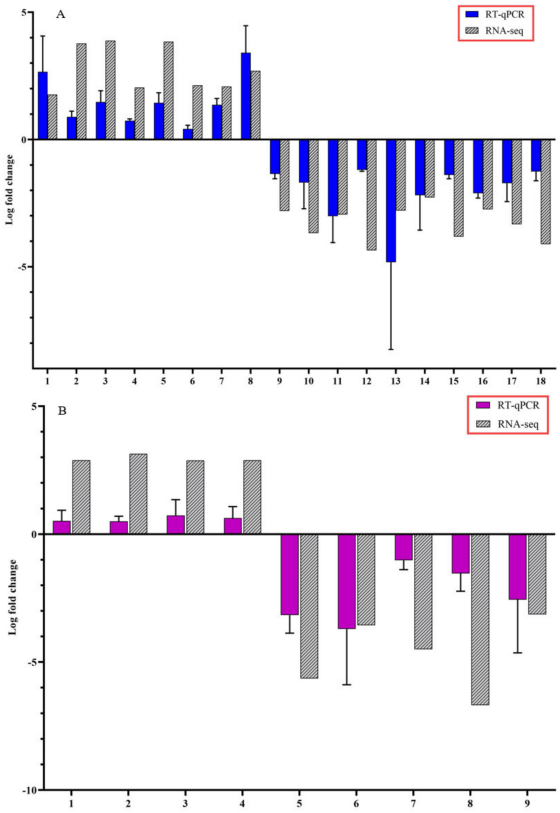

Figure 5. Expression pattern validation of selected candidate differentially expressed genes (DEGs) by reverse transcription-quantitative polymerase chain reaction (RT-qPCR) on stems and roots of citrus dwarfing viroid (CDVd) infected relative to non-infected citrus trees. The relative gene expression was evaluated by the comparative Cq method using actin as a reference gene. The targeted DEGs used in the analysis for stems (**A**) were: (1) receptor-like protein 9DC3 (LOC102630240); (2) germin-like protein subfamily T member (LOC102611719); (3) pentatricopeptide repeat-containing protein At2g17525 (LOC102610118); (4) MADS-box transcription factor 23-like (LOC102630220); (5) phospholipase A1-Ibeta2 (LOC102609966); (6) protein TIC 55 (LOC102614849); (7) pentatricopeptide repeat-containing protein At1g08070 (LOC102619843); (8) transcription factor MYB13 (LOC102616893); (9) SKP1-like protein 21 (LOC102620512); (10) amino-acid permease BAT1-like (LOC102620992); (11) LOC102627502 pentatricopeptide repeat-containing protein At4g21300; (12) uncharacterized protein (LOC102608277); (13) protein SHORT-ROOT-like (LOC102610900); (14) protein IQ-DOMAIN 1, transcript variant X1 (LOC102628194); (15) hydroxyproline O-galactosyltransferase GALT3, transcript variant X3 (LOC102626136); (16) cytochrome P450 82C4-like; (17) LOC102622795 thaumatin-like protein 1 (LOC102619709); (18) Plant uncharacterized (LOC102625692). Targeted DEGs used in the analysis for the roots (**B**) were: (1) Plant invertase/pectin methylesterase inhibitor superfamily protein (Ptrif.0009s1914.1); (2) S-adenosyl-L-methionine-dependent O-methyltransferase/ethylene-responsive transcription factor ERF114 (Ptrif.0005s1389.1); (3) C2H2-like zinc finger protein (Ptrif.0005s2465.1); (4) Pentatricopeptide repeat (PPR) superfamily protein (Ptrif.0006s1595.1); (5) Kinase-inducible domain interacting 9 (Ptrif.0001s0240.1); (6) Pentatricopeptide repeat (PPR-like) superfamily protein (Ptrif.0003s3971.1); (7) zinc-finger protein 10 (Ptrif.0006s0692.1); (8) Calcium-dependent lipid-binding (CaLB domain) family protein (Ptrif.0003s4060.1); (9) GNS1/SUR4 membrane protein family (Ptrif.0005s2586.1). Error bars for the RT-qPCR are standard deviations.

3.4. Functional Classification of DEGs

The RNA-seq data were annotated based on the gene ontology (GO) terms, which categorized the DEGs in response to CDVd infection for both stems and roots into various biological, molecular, and cellular processes (Figure 6). Among the upregulated DEGs in the stems, there were 143 associated with biological process (BP), 82 with molecular function (MF), and 614 with cellular component (CC). Within the downregulated DEGs in the stems, 143 were associated with BP, 84 with MF, and 54 with CC. The top stem DEGs categorized in BP were (i) metabolic process (up 38 and down 29); (ii) cellular process (up 36 and down 46) (iii) Biological regulation (up 13 and down 12). For stem DEGs associated with MP (i) catalytic activity (up 42 and down 29); (ii) binding (up and down 33); (iii) transport activity (down 11 and up 1). Stem DEGs that belong to the CC were (i) cellular anatomical entities (up 51 and down 52) and (ii) protein-containing complexes (up 10 and down 2) (Figure 6A). A list of all GO term annotations for the stem DEGs can be found in Supplementary Tables S6 and S7.

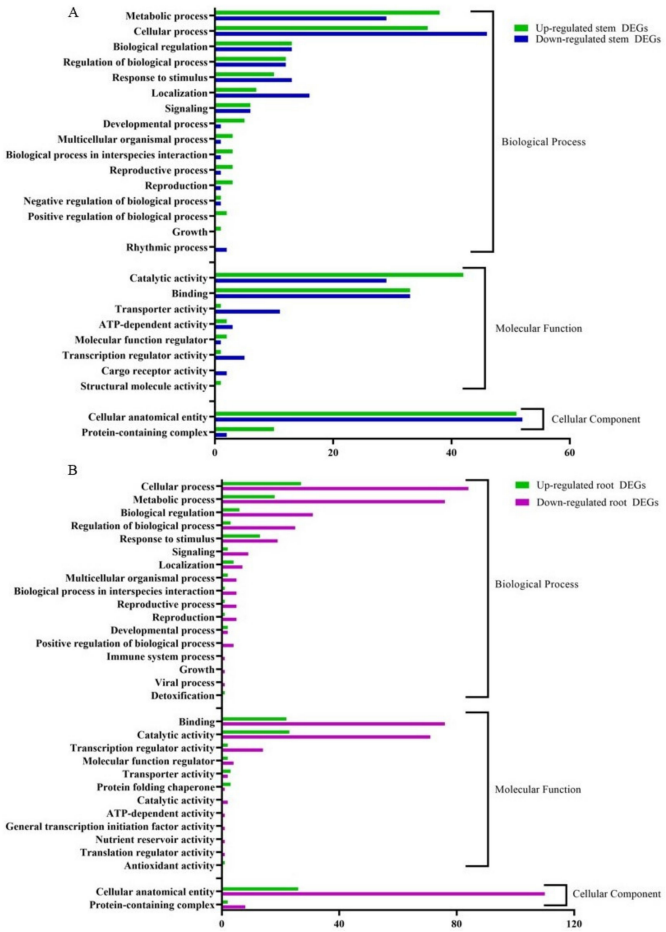

Figure 6. Clusters of orthologous groups functional classification of differentially expressed genes (DEGs), between non-infected and citrus dwarfing viroid (CDVd)-infected (**A**) stem and (**B**) root tissues. The bar graph shows the number of sequences and distribution in different functional categories of the predicted targets at gene ontology (GO) level 2.

From the upregulated DEGs identified in the roots, there were 81 associated with BP, 56 with MF, and 28 CC. Among the downregulated root DEGs, 280 were associated with BP, 174 with MF, and 118 CC. The top root DEGs in BP were categorized into (i) cellular process (up 27 and down 84), (ii) metabolic process (up 18 and down 76), and (iii) Biological regulation (up 6 and down 31). The top root DEGs in MF were associated with (i) binding (up 22 and down 76); (ii) catalytic activity (up 23 and down 71); (iii) transcription regulatory

activity (up 2 and down 14). Only two GO terms were associated with CC (i) cellar anatomical entity (up 26 and down 110) and (ii) protein-containing complex (up 2 and down 8) (Figure 6B). A list of all GO term annotations for the root DEGs can be found in Supplementary Tables S8 and S9.

Kyoto Encyclopedia of Genes and Genome (KEGG) analysis was performed on up- and downregulated DEGs from non-infected and CDVd-infected trees from the stem and root tissues (Figure 7). The KEGG results for stem upregulated DEGs identified 82 pathways and 25 sequences linked to specific pathways. The pathways with the most sequences from upregulated stem DEGs were starch and sucrose metabolism (3) (ko00500), NOD-like receptor signaling pathway (2) (ko04621), tryptophan metabolism (2) (ko00980), and protein processing in the endoplasmic reticulum (2) (ko04141). KEGG analysis also identified 96 pathways and 25 sequences in stem downregulated DEGs, with the highest downregulated pathway being the plant circadian rhythm (3) (ko04712) (Figure 7A). KEGG analysis for roots upregulated DEGs found 73 pathways and 26 sequences and 118 pathways and 53 sequences from downregulated roots. The highest number of sequences associated with upregulated roots were protein processing in the endoplasmic reticulum (10 sequences) (ko04141). In contrast to the downregulated roots, the NOD-like receptor signaling pathway (ko04621) (7), MAPK signaling pathway (7) (ko04010), and plant hormone signal transduction (5) (ko04075) were the highest (Figure 7B). A complete list of all KEGG results can be found in Supplementary Tables S10–S13.

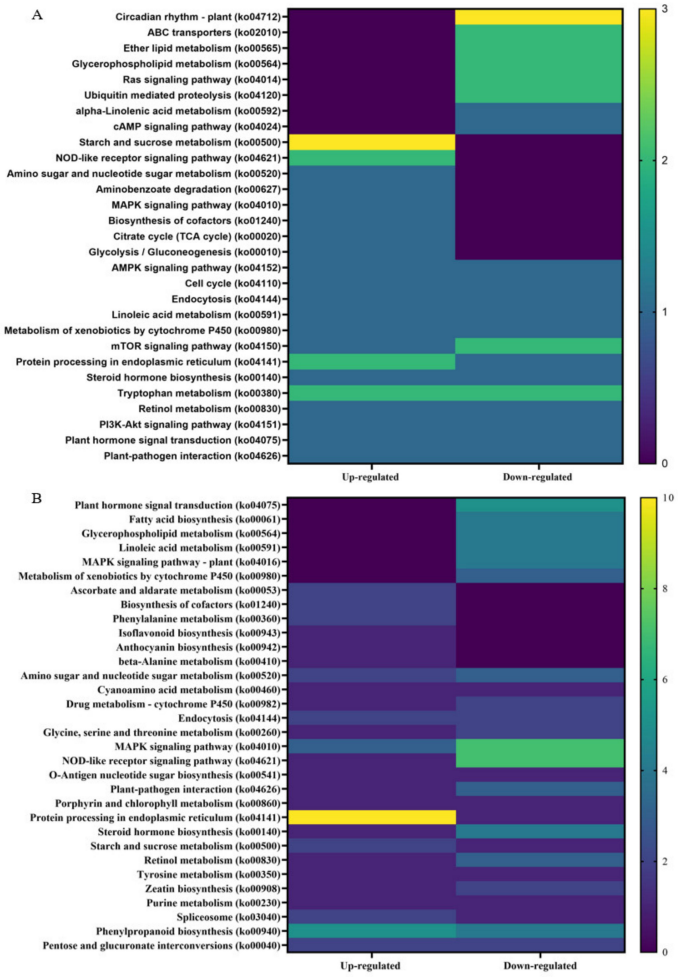

Figure 7. Distribution of Kyoto Encyclopedia of Genes and Genomes (KEGG) pathway classification of upregulated differentially expressed genes (DEGs) between non-infected and citrus dwarfing viroid (CDVd)-infected (**A**) stem and (**B**) root tissues. The heat map shows the KEGG function and the number of associated sequences.

4. Discussion

Citrus is among the most economically valuable fruit crops. In 2019, citrus production exceeded 157.9 million tons in over 9.8 million hectares worldwide [1]. The ever-reducing global natural resources (i.e., decreased arable land and water availability) combined with climate change, agricultural labor shortages, and the increased disease pressure of deadly citrus diseases such as HLB demand the adoption of novel citriculture practices. High-density citrus plantings, the possible implementation of mechanized citrus harvest, and citrus production under protective structures are some of the most promising trends for sustainable citriculture. The ability to produce dwarf citrus trees is critical for implementing these innovations and maximizing returns on investments [19,42–46].

Dwarfed sweet orange trees propagated on trifoliate orange rootstock, where reduced vegetative growth is achieved without compromising fruit yield or quality, have been produced using CDVd. CDVd is part of a group of so-called "graft-transmissible dwarfing agents," the use of which has been explored for almost fifty years since it was initially proposed [16,18,47–50]. Previously, we observed CDVd significantly reduced sweet orange canopy volume on trifoliate rootstock by reducing vegetative growth [19–21]. Long-term field observations indicated that CDVd might be used as a possible tool for high-density plantings of citrus. In addition, key findings on the possible biological mechanism through which CDVd affects specific rootstock scion combinations to reduce tree canopy volume were obtained [14]. Understanding the detailed molecular mechanisms leading to reduced canopy volume of commercial citrus tree varieties in response to CDVd infection is critical. Indeed, it would provide the information to produce reduced-size citrus trees without a graft-transmissible viroid agent.

Transcriptomic profiling provides a rapid and cost-effective approach to identifying target genes responsible for the observed reduced vegetative growth of CDVd-infected sweet orange trees. Commercial field citrus trees consist of two different species: the scion, producing the canopy of the tree (i.e., branches, stems, and leaves), and the rootstock, from which the root system of the tree (i.e., taproot, lateral, and feeder roots) develops [51]; therefore, any observed tree phenotype is a result of gene expression not in one but two species that closely interact with each other. In this study, we performed a transcriptome analysis of CDVd-infected stems and roots from sweet orange on trifoliate rootstock trees grown in high-density plantings and compared them with non–infected controls. Here, we showed that CDVd infection affects a wide range of biological functions via different stem and root mRNA transcripts. Furthermore, it complements recent molecular studies targeting CDVd-derived small RNAs on dwarfed citrus [32]. As a result of differential expression analysis, a total of 409 CDVd-dependent differentially expressed genes (DEGs) were deregulated (131 upregulated and 278 downregulated), with the majority of upregulated genes in the stems (83/131), and most downregulated genes in the roots (186/278) (Table 2).

The five most significant upregulated genes in CDVd-infected stems include: LOC102607140, a probable 28S rRNA (cytosine-C(5))-methyltransferase, an ortholog of the *Arabidopsis thaliana* (AT5G26180), which plays a role in regulating translation in response to stress [52]; LOC102611719, a germin-like protein subfamily T member. Germin-like proteins (GLPs) are encoded by multigene families in several plant species, and some subfamily members play a role in defense against pathogen attack [53,54]; LOC102610118, a pentatricopeptide repeat-containing protein (ortholog of AT2g17525). Pentatricopeptide repeat (PPR) proteins belong to a large gene family in plants. Some PPR proteins play important roles in organellar RNA metabolism and organ development in Arabidopsis and rice, while their functions remain unknown in woody species [55]; LOC102616051, cytosolic sulfotransferase 15-like, an ortholog of the Arabidopsis cytosolic sulfotransferase genes. In Arabidopsis, a hydroxyjasmonate sulfotransferase was reported to participate in the hydroxylation and sulfonation reactions that might be components of a pathway that inactivates excess jasmonic acid in plants [56]. The LOC102614284 is associated with aspartic proteinase Asp1-like, and plant aspartic proteinases have been implicated in diverse cellular functions, including protein

processing and/or degradation, plant senescence, stress responses, programmed cell death, and reproduction [57].

The five most significantly downregulated genes in CDVd-infected stems include: LOC102627502, a pentatricopeptide repeat-containing protein, an ortholog of At4g21300; LOC102620512, SKP1-like protein 21, which is involved in ubiquitination and subsequent proteasomal degradation of target proteins [58]; LOC102610900, SHORT-ROOT-like protein, which controls radial patterning of the Arabidopsis root, and therefore root growth [59], which is consistent with reduced root mass in viroid infected plants [9]; LOC102620992, an amino-acid permease BAT1-like, which plays a role in primary carbon metabolism and plant growth by mediating the transport of gamma amino butyric acid from the cytosol to mitochondria in Arabidopsis [60]; LOC102628393, serine/threonine-protein kinase ATG1a, involved in autophagy in a nutritional condition-dependent manner [61].

In CDVd-infected roots, the five most significantly upregulated genes include: Ptrif.0009s1914.1 (ortholog of AT5G62350/LOC_Os06g49760), a plant invertase/pectin methylesterase inhibitor superfamily protein, which inhibits pectin methylesterases (PMEs) and invertases (PMIs) and has been implicated in the regulation of fruit development, carbohydrate metabolism, and cell wall extension as well as inhibition of microbial pathogen PMEs. The interplay between PME and PMEI is a determinant of cell adhesion, cell wall porosity, and elasticity, as well as a source of signaling molecules released upon cell wall stress [62]. The Ptrif.0004s1154.1 (ortholog of AT5G07310/Cre14.g620500/LOC_Os04g32620) is an integrase-type DNA-binding superfamily protein involved in the regulation of transcription and recently reported to integrate the jasmonate and cytokinin signaling pathways to repress adventitious rooting in Arabidopsis [63]; Ptrif.0005s1389.1, an ortholog of Cre05.g240400/LOC_Os12g25450, S-adenosyl-L-methionine-dependent O-methyltransferase/ethylene-responsive transcription factor, which methylates proteins, small molecules, lipids, and nucleic acids [64]; Ptrif.0005s2465.1 (ortholog of AT5G52010/LOC_Os06g07020) C2H2-like zinc finger protein, which contains one of the most common domains found in the transcription factors of higher eukaryotes [65]; and Ptrif.0006s1595.1 (ortholog of AT5G03800) another pentatricopeptide repeat (PPR) superfamily protein.

The five most significantly downregulated genes in CDVd-infected roots include: Ptrif.0001s0240.1 (ortholog of AT4G32295), which in Arabidopsis is part of a transcriptional repressor complex that regulates leaf growth [66]; Ptrif.0003s0980.2, (ortholog of LOC_Os04g48160) a putative IQ calmodulin-binding motif family protein; Ptrif.0006s0692.1, an ortholog of AT2G37740/LOC_Os05g20930, zinc-finger protein 10, a transcription factor that may regulate cell division and growth [67]; Ptrif.0003s4060.1 (ortholog of AT4G01200) a calcium-dependent lipid-binding (CaLB domain) family protein, a repressor of abiotic stress responses in Arabidopsis [68]; and Ptrif.0005s2586.1 (ortholog of AT1G75000/LOC_Os12g43890) a GNS1/SUR4 membrane protein family, enzymes related to very long-chain fatty acid synthesis in Arabidopsis [69].

Among the additional interesting CDVd-responsive stem genes whose differential expression was verified by RT-qPCR (Figure 5A), several were found including the plant defense receptor-like protein 9DC3 (LOC102630240) [70]; the MADS-box transcription factor 23-like (LOC102630220) [71], which is part of the transcription factor (TF) families (WRKY, MADS-box and MYB) that activate unique abiotic and biotic stress-responsive strategies considered as key determinants for defense and developmental processes in most eukaryotic plants [72]; the phospholipase A1-Ibeta2 (LOC102609966) [73], the chloroplast import protein TIC 55 (LOC102614849), the chloroplast import protein [74]; the chloroplast pentatricopeptide repeat-containing protein ortholog of At1g08070 (LOC102619843), which is involved in RNA editing events within the chloroplast [75]; the transcription factor MYB13 (LOC102616893), which regulates meristem function by being a component of a regulatory network controlling the establishment and/or development of the shoot system in Arabidopsis [76]; protein IQ-DOMAIN 1, transcript variant X1 (LOC102628194) which plays a role with calmodulins or calmodulin-like proteins as well as involved in scaffolding in cellular signaling and trafficking [77,78]; hydroxyproline O-galactosyltransferase GALT3,

transcript variant X3 (LOC102626136), which commits arabinogalactan proteins to the first step in arabinogalactan polysaccharide addition. AGP glycans play essential roles in both vegetative and reproductive plant growth [79]; cytochrome P450 82C4-like, which is involved in the early Fe deficiency response in Arabidopsis [80]; LOC102622795; thaumatin-like protein 1 (LOC102619709), involved in local responses of roots to colonization by non-pathogenic plant growth-promoting rhizobacteria [81].

In roots, CDVd-responsive genes verified by RT-qPCR included integrase-type DNA-binding superfamily protein (Ptrif0004s1154.1), involved in transcriptional regulation S-adenosyl-L-methionine-dependent O-methyltransferase/ethylene-responsive transcription factor ERF114 (Ptrif.0005s1389.1), involved in shoot development and architecture in Arabidopsis [82,83]; and the zinc-finger protein 10 (Ptrif.0006s0692.1), the overexpression of which was associated with dwarf plants in Arabidopsis [67]. Calcium-dependent lipid-binding (CaLB domain) family protein (Ptrif.0003s4060.1). Stress affects cell ion homeostasis, and plants adjust it by regulating membrane transporters and channels. Ca2+ is key in such a process as it regulates the protein kinases and phosphatases that control ion transport activity in response to environmental stimuli [84] (Supplementary Table S5).

Gene ontology (GO) assignments were used to classify the function of the identified DEGs. GO term enrichment analysis showed that in both stems and roots of CDVd-infected trees, for the biological process category, the GO terms corresponding to metabolic process and cellular process were the most enriched terms in response to CDVd; for molecular function, the catalytic activity and binding are the most enriched, and for the cellular component category, the cellular anatomical entity term was most enriched in the stems (Figure 6A,B).

In order to gain further insight into the function of DEGs correlating to a reduced vegetative growth as observed in CDVd-infected trees, the KEGG pathway classification was performed. Overall, circadian rhythms (ko04712), starch and sucrose metabolism (ko00500), and protein processing in the endoplasmic reticulum (ko04141) were most altered in response to CDVd infection. Circadian rhythms (ko04712), downregulated in CDVd-infected stems, are known to cross-talk with defense signaling against bacteria in plants [85] and to be important determinants in the outcome of plant-pathogen interactions [86]. Starch and sucrose metabolism (ko00500) were upregulated in both CDVd-infected stems and roots. Sucrose, the main form of assimilated carbon produced during photosynthesis, has important roles as a signaling molecule, and it is involved in many metabolic processes in plants; it is essential for plant growth and development and plays a role in plant defense by activating plant immune responses against pathogens. Upon infection, pathogens hijack the plant metabolism to access the plant sugars and, in doing so, trigger plant defense responses. Invertases appear to be involved in establishing plant defense responses [87].

Protein processing in the endoplasmic reticulum (ko04141) was upregulated in roots and stems, consistent with higher metabolic activity levels. Tryptophan metabolism (ko00380) was up- and downregulated in stems. Tyrosine and tryptophan are precursors for the plant defense compounds dhurrin and indole glucosinolates, respectively. In addition, tryptophan is a precursor for the essential phytohormone indole-3-acetic acid [88]. Other KEGG pathway classification terms that were altered in response to CDVd infection include: Lipid metabolism (glycerophospholipid (ko00564), which was downregulated in roots and stems; ether lipid (ko00565) was downregulated in stems; ABC transporters (ko 02010), Ras signaling pathway, mTOR signaling pathway (ko04150), which were downregulated in stems.

To date, only one previous citrus gene expression profiling study in response to CDVd infection has been reported [22], and it differs from ours in many important aspects. Indeed, it predates the widespread use of HTS applications and the availability of reference genomes for *C. sinensis* and *P. trifoliata*. Instead, the authors profiled the transcriptome using the differential display technique (DDRT-PCR). Most importantly, however, the authors studied the sensitive viroid bioindicator 'Etrog' citron, Arizona 861-S1, newly inoculated with CDVd (18 months old) grown under growth chamber conditions and

expressing symptoms of leaf drooping and petiole necrosis. Provided these experimental conditions, as expected, among the upregulated genes, a suppressor of RNA silencing was identified [22]. In contrast, our study used HTS technologies to analyze 18-year-old, field-grown commercial citrus tree varieties that do not express typical viroid symptoms of leaf epinasty and midvein and petiole necrosis [89]. Therefore, it is not surprising that the transcriptome profiling was different.

When taken together, our results indicate that CDVd modulates the expression profile of important citrus growth and developmental processes that may participate in the cellular changes leading to the observed phenotype of reduced vegetative growth and overall smaller tree size. In this study, most of the transcriptome expression reprogramming appeared to occur in the stems (*C. sinensis*) rather than in the roots (*C. trifoliata*), which is consistent with the phenotypic observation of the reduced stem vegetative growth of the stems and striking dwarfed citrus tree phenotype in CDVd-infected trees [21]. It is also in agreement with the observation that the trifoliate orange rootstock does not display major symptoms in response to CDVd infection [90–92]. Even though our study demonstrates the potential use of modern molecular technologies to decipher complex plant responses to biotic factors using plants growing in agricultural production systems, future studies employing transgenics and model plant systems could provide additional evidence to dissect further the genes and pathways participating in the development of the dwarf phenotype identified in this study.

Lastly, the lack of major alterations in the pathogen defense transcriptome profile in our study is in contrast to studies with other viroids that demonstrated altered expression of plant defense genes [11,24]. This finding supports the idea that when viroid RNAs such as CDVd are used for horticultural purposes, such as reducing tree canopy volume, perhaps they are better described as "Transmissible small nuclear ribonucleic acids" (TsnRNAs). This term provides a more detailed description of the TsnRNA's hallmark properties (i.e., transmissibility, small genome size, site of replication, and RNA nature) as well as dissociation from a generic virology term, such as "viroid", which implies disease and crop loss. Therefore TsnRNAs that do not express a disease syndrome but rather act as modifying agents of tree performance resulting in desirable agronomic traits, such as reduced tree size for high-density plantings with potential economic and sustainability advantages, can be distinguished from the pathogenic viroids [18,20].

Supplementary Materials: The following are available online at: https://www.mdpi.com/article/10.3390/microorganisms10061144/s1, Table S1: List of primers used for RT-qPCR relative quantification of mRNA target genes; Table S2: List of upregulated DEGs identified in stem (*Citrus sinensis* (L.) Osbeck) tissue; Table S3: List of downregulated DEGs identified in stem (*Citrus sinensis* (L.) Osbeck) tissue; Table S4: List of upregulated DEGs identified in root (*Citrus trifoliata* (L.)) tissue; Table S5: List of downregulated DEGs identified in root (*Citrus trifoliata* (L.)) tissue; Table S6: List of GO terms for upregulated DEGs identified in stem (*Citrus sinensis* (L.) Osbeck) tissue; Table S7: List of GO terms for downregulated DEGs identified in stem (*Citrus sinensis* (L.) Osbeck) tissue; Table S8: List of GO terms for upregulated DEGs identified in root (*Citrus trifoliata* (L.)) tissue; Table S9: List of GO terms for downregulated DEGs identified in root (*Citrus trifoliata* (L.)) tissue; Table S10: List of KEGG for upregulated DEGs identified in stem (*Citrus sinensis* (L.) Osbeck) tissue; Table S11: List of KEGG for downregulated DEGs identified in stem (*Citrus sinensis* (L.) Osbeck) tissue; Table S12: List of KEGG for upregulated DEGs identified in root (*Citrus trifoliata* (L.)) tissue; Table S13: List of KEGG for downregulated DEGs identified in root (*Citrus trifoliata* (L.)) tissue.

Author Contributions: I.L.-C., T.D. and G.V. conceived and designed the experiments, analyzed the data, and wrote the manuscript. T.D. and I.L.-C. performed the experiments with the assistance of S.C., F.O. and S.B. All authors contributed to the article and approved the submitted version. All authors have read and agreed to the published version of the manuscript.

Funding: This research was funded by the Citrus Research Board project "Citrus Dwarfing of Commercial Varieties using TsnRNAs" (project 5100-154) awarded to GV. Support was provided in part by the Citrus Research Board (project 6100), the USDA National Institute of Food and Agriculture, Hatch project 1020106.

Data Availability Statement: The dataset presented in this study can be found in NCBI Sequence Read Archive under the accession numbers SAMN26677719 to SAMN26677722.

Acknowledgments: We would like to acknowledge the assistance of the dedicated personnel of the CCPP and the UC-ANR Lindcove Research and Extension Center. Mention of trade names or commercial products in this publication is solely for the purpose of providing specific information and does not imply recommendation or endorsement by the University of California. UC is an equal opportunity provider and employer. The authors are acknowledging the Cahuilla people as the Traditional Custodians of the Land on which the experimental work was completed.

Conflicts of Interest: The authors declare no conflict of interest.

References

1. Babcock, B.A. Economic Impact of California's Citrus Industry in 2020. *J. Citrus Pathol.* **2022**, *9*. [CrossRef]
2. Van Duyn, M.A.; Pivonka, E. Overview of the Health Benefits of Fruit and Vegetable Consumption for the Dietetics Professional: Selected Literature. *J. Am. Diet. Assoc.* **2000**, *100*, 1511–1521. [CrossRef]
3. Yao, L.H.; Jiang, Y.M.; Shi, J.; Tomás-Barberán, F.A.; Datta, N.; Singanusong, R.; Chen, S.S. Flavonoids in Food and Their Health Benefits. *Plant Foods Hum. Nutr.* **2004**, *59*, 113–122. [CrossRef] [PubMed]
4. Boswell, S.B. Others Tree Spacing of'Washington'navel Orange. *J. Am. Soc. Hortic. Sci.* **1970**, *95*, 523–528.
5. Platt, R.G. Treatment of Frost-Inured Citrus, Avocados. *Calif. Citrogr.* **1973**, *113–114*, 140.
6. Tucker, D.P.H.; Wheaton, T.A. Trends in Higher Citrus Planting Densities. *Proc. Fla. State Hort. Soc.* **1978**, *91*, 36–40.
7. Schumann, A.W.; Singerman, A.; Wright, A.L.; Ferrarezi, R.S. Citrus under Protective Screen (CUPS) Production Systems. In *Citrus under Protective Screen (CUPS) Production Systems*; University of Florida Entomology and Nematology Department, UF/IFAS Extension: Gainesville, FL, USA, 2017.
8. Flores, R.; Hernández, C.; Martínez de Alba, A.E.; Daròs, J.-A.; Di Serio, F. Viroids and Viroid-Host Interactions. *Annu. Rev. Phytopathol.* **2005**, *43*, 117–139. [CrossRef]
9. Murcia, N.; Hashemian, S.M.B.; Serra, P.; Pina, J.A.; Duran-Vila, N. Citrus Viroids: Symptom Expression and Performance of Washington Navel Sweet Orange Trees Grafted on Carrizo Citrange. *Plant Dis.* **2015**, *99*, 125–136. [CrossRef]
10. Navarro, B.; Flores, R.; Di Serio, F. Advances in Viroid-Host Interactions. *Annu. Rev. Virol.* **2021**, *8*, 305–325. [CrossRef]
11. Itaya, A.; Matsuda, Y.; Gonzales, R.A.; Nelson, R.S.; Ding, B. Potato Spindle Tuber Viroid Strains of Different Pathogenicity Induces and Suppresses Expression of Common and Unique Genes in Infected Tomato. *Mol. Plant. Microbe Interact.* **2002**, *15*, 990–999. [CrossRef]
12. Rodio, M.-E.; Delgado, S.; De Stradis, A.; Gómez, M.-D.; Flores, R.; Di Serio, F. A Viroid RNA with a Specific Structural Motif Inhibits Chloroplast Development. *Plant Cell* **2007**, *19*, 3610–3626. [CrossRef]
13. Owens, R.A.; Tech, K.B.; Shao, J.Y.; Sano, T.; Baker, C.J. Global Analysis of Tomato Gene Expression during Potato Spindle Tuber Viroid Infection Reveals a Complex Array of Changes Affecting Hormone Signaling. *Mol. Plant. Microbe Interact.* **2012**, *25*, 582–598. [CrossRef]
14. Gillings, M.R.; Broadbent, P.; Gollnow, B.I. Viroids in Australian Citrus: Relationship to Exocortis, Cachexia and Citrus Dwarfing. *Funct. Plant Biol.* **1991**, *18*, 559–570. [CrossRef]
15. Hadas, R.; Bar-Joseph, M. Variation in Tree Size and Rootstock Scaling of Grapefruit Trees Inoculated with a Complex of Citrus Viroids. In *International Organization of Citrus Virologists Conference Proceedings (1957–2010)*; IOCV: Riverside, CA, USA, 1991; Volume 11, pp. 240–243. [CrossRef]
16. Hutton, R.J.; Broadbent, P.; Bevington, K.B. Viroid Dwarfing for High Density Citrus Plantings. In *Horticultural Reviews*; John Wiley and Sons, Inc.: Hoboken, NJ, USA, 2000; Volume 24, pp. 277–317. ISBN 9780471333746.
17. Semancik, J.S.; Bash, J.; Gumpf, D.J. Induced Dwarfing of Citrus by Transmissible Small Nuclear RNA (TsnRNA). In *International Organization of Citrus Virologists Conference Proceedings (1957–2010)*; IOCV: Riverside, CA, USA, 2002; Volume 15, pp. 390–394. [CrossRef]
18. Semancik, J.S. *Considerations for the Introduction of Viroids*; Hadidi, A., Flores, R., Randles, J.W., Semancik, J.S., Eds.; CSIRO Publishing: Clayton, VIC, Australia, 2003; pp. 357–362.
19. Vidalakis, G.; Pagliaccia, D.; Bash, J.A.; Afunian, M.; Semancik, J.S. Citrus Dwarfing Viroid: Effects on Tree Size and Scion Performance Specific to Poncirus Trifoliata Rootstock for High-Density Planting. *Ann. Appl. Biol.* **2011**, *158*, 204–217. [CrossRef]
20. Semancik, J.S.; Rakowski, A.G.; Bash, J.A.; Gumpf, D.J. Application of Selected Viroids for Dwarfing and Enhancement of Production of 'Valencia' Orange. *J. Hortic. Sci.* **1997**, *72*, 563–570. [CrossRef]
21. Lavagi-Craddock, I.; Campos, R.; Pagliaccia, D.; Kapaun, T.; Lovatt, C.; Vidalakis, G. Citrus Dwarfing Viroid Reduces Canopy Volume by Affecting Shoot Apical Growth of Navel Orange Trees Grown on Trifoliate Orange Rootstock. *J. Citrus Pathol.* **2020**, *7*, 1–6. [CrossRef]
22. Tessitori, M.; Maria, G.; Capasso, C.; Catara, G.; Rizza, S.; De Luca, V.; Catara, A.; Capasso, A.; Carginale, V. Differential Display Analysis of Gene Expression in Etrog Citron Leaves Infected by Citrus Viroid III. *Biochim. Biophys. Acta BBA Gene Struct. Expr.* **2007**, *1769*, 228–235. [CrossRef]

23. Wang, Y.; Wu, J.; Qiu, Y.; Atta, S.; Zhou, C.; Cao, M. Global Transcriptomic Analysis Reveals Insights into the Response of "Etrog" Citron (*Citrus medica* L.) to Citrus Exocortis Viroid Infection. *Viruses* **2019**, *11*, 453. [CrossRef]
24. Olivier, T.; Bragard, C. Innate Immunity Activation and RNAi Interplay in Citrus Exocortis Viroid—Tomato Pathosystem. *Viruses* **2018**, *10*, 587. [CrossRef]
25. Cottilli, P.; Belda-Palazón, B.; Adkar-Purushothama, C.R.; Perreault, J.-P.; Schleiff, E.; Rodrigo, I.; Ferrando, A.; Lisón, P. Citrus Exocortis Viroid Causes Ribosomal Stress in Tomato Plants. *Nucleic Acids Res.* **2019**, *47*, 8649–8661. [CrossRef]
26. Xu, Q.; Chen, L.-L.; Ruan, X.; Chen, D.; Zhu, A.; Chen, C.; Bertrand, D.; Jiao, W.-B.; Hao, B.-H.; Lyon, M.P.; et al. The Draft Genome of Sweet Orange (*Citrus sinensis*). *Nat. Genet.* **2013**, *45*, 59–66. [CrossRef]
27. Martinelli, F.; Uratsu, S.L.; Albrecht, U.; Reagan, R.L.; Phu, M.L.; Britton, M.; Buffalo, V.; Fass, J.; Leicht, E.; Zhao, W.; et al. Transcriptome Profiling of Citrus Fruit Response to Huanglongbing Disease. *PLoS ONE* **2012**, *7*, e38039. [CrossRef]
28. Fu, S.; Shao, J.; Zhou, C.; Hartung, J.S. Transcriptome Analysis of Sweet Orange Trees Infected with "Candidatus Liberibacter Asiaticus" and Two Strains of Citrus Tristeza Virus. *BMC Genom.* **2016**, *17*, 349. [CrossRef]
29. Wang, Y.; Zhou, L.; Yu, X.; Stover, E.; Luo, F.; Duan, Y. Transcriptome Profiling of Huanglongbing (HLB) Tolerant and Susceptible Citrus Plants Reveals the Role of Basal Resistance in HLB Tolerance. *Front. Plant Sci.* **2016**, *7*, 933. [CrossRef]
30. Arce-Leal, Á.P.; Bautista, R.; Rodríguez-Negrete, E.A.; Manzanilla-Ramírez, M.Á.; Velázquez-Monreal, J.J.; Santos-Cervantes, M.E.; Méndez-Lozano, J.; Beuzón, C.R.; Bejarano, E.R.; Castillo, A.G.; et al. Gene Expression Profile of Mexican Lime (*Citrus aurantifolia*) Trees in Response to Huanglongbing Disease Caused by Candidatus Liberibacter Asiaticus. *Microorganisms* **2020**, *8*, 528. [CrossRef]
31. Visser, M.; Cook, G.; Burger, J.T.; Maree, H.J. In Silico Analysis of the Grapefruit SRNAome, Transcriptome and Gene Regulation in Response to CTV-CDVd Co-Infection. *Virol. J.* **2017**, *14*, 200. [CrossRef]
32. Dang, T.; Lavagi-Craddock, I.; Bodaghi, S.; Vidalakis, G. Next-Generation Sequencing Identification and Characterization of MicroRNAs in Dwarfed Citrus Trees Infected with Citrus Dwarfing Viroid in High-Density Plantings. *Front. Microbiol.* **2021**, *12*, 646273. [CrossRef]
33. Peng, Z.; Bredeson, J.V.; Wu, G.A.; Shu, S.; Rawat, N.; Du, D.; Parajuli, S.; Yu, Q.; You, Q.; Rokhsar, D.S.; et al. A Chromosome-Scale Reference Genome of Trifoliate Orange (*Poncirus trifoliata*) Provides Insights into Disease Resistance, Cold Tolerance and Genome Evolution in Citrus. *Plant J.* **2020**, *104*, 1215–1232. [CrossRef] [PubMed]
34. Dobin, A.; Davis, C.A.; Schlesinger, F.; Drenkow, J.; Zaleski, C.; Jha, S.; Batut, P.; Chaisson, M.; Gingeras, T.R. STAR: Ultrafast Universal RNA-Seq Aligner. *Bioinformatics* **2013**, *29*, 15–21. [CrossRef] [PubMed]
35. Anders, S.; Pyl, P.T.; Huber, W. HTSeq—A Python Framework to Work with High-Throughput Sequencing Data. *Bioinformatics* **2015**, *31*, 166–169. [CrossRef] [PubMed]
36. Robinson, M.D.; McCarthy, D.J.; Smyth, G.K. EdgeR: A Bioconductor Package for Differential Expression Analysis of Digital Gene Expression Data. *Bioinformatics* **2010**, *26*, 139–140. [CrossRef]
37. Götz, S.; García-Gómez, J.M.; Terol, J.; Williams, T.D.; Nagaraj, S.H.; Nueda, M.J.; Robles, M.; Talón, M.; Dopazo, J.; Conesa, A. High-Throughput Functional Annotation and Data Mining with the Blast2GO Suite. *Nucleic Acids Res.* **2008**, *36*, 3420–3435. [CrossRef]
38. Altschul, S.F.; Gish, W.; Miller, W.; Myers, E.W.; Lipman, D.J. Basic Local Alignment Search Tool. *J. Mol. Biol.* **1990**, *215*, 403–410. [CrossRef]
39. Kanehisa, M.; Goto, S. KEGG: Kyoto Encyclopedia of Genes and Genomes. *Nucleic Acids Res.* **2000**, *28*, 27–30. [CrossRef]
40. Hunter, S.; Apweiler, R.; Attwood, T.K.; Bairoch, A.; Bateman, A.; Binns, D.; Bork, P.; Das, U.; Daugherty, L.; Duquenne, L.; et al. InterPro: The Integrative Protein Signature Database. *Nucleic Acids Res.* **2009**, *37*, D211–D215. [CrossRef]
41. Bustin, S.A.; Benes, V.; Garson, J.A.; Hellemans, J.; Huggett, J.; Kubista, M.; Mueller, R.; Nolan, T.; Pfaffl, M.W.; Shipley, G.L.; et al. The MIQE Guidelines: Minimum Information for Publication of Quantitative Real-Time PCR Experiments. *Clin. Chem.* **2009**, *55*, 611–622. [CrossRef]
42. Stover, E.; Castle, W.S.; Spyke, P. The Citrus Grove of the Future and Its Implications for Huanglongbing Management. *Proc. Fla. State Hort. Soc.* **2008**, *121*, 155–159.
43. Gottwald Current Epidemiological Understanding of Citrus Huanglongbing. *Annu. Rev. Phytopathol.* **2010**, *48*, 119–139. [CrossRef]
44. Lambin, E.F. Global Land Availability: Malthus versus Ricardo. *Glob. Food Secur.* **2012**, *1*, 83–87. [CrossRef]
45. Verburg, P.H.; Mertz, O.; Erb, K.-H.; Haberl, H.; Wu, W. Land System Change and Food Security: Towards Multi-Scale Land System Solutions. *Curr. Opin. Environ. Sustain.* **2013**, *5*, 494–502. [CrossRef]
46. da Graça, J.V.; Douhan, G.W.; Halbert, S.E.; Keremane, M.L.; Lee, R.F.; Vidalakis, G.; Zhao, H. Huanglongbing: An Overview of a Complex Pathosystem Ravaging the World's Citrus. *J. Integr. Plant Biol.* **2016**, *58*, 373–387. [CrossRef]
47. Cohen, M. Exocortis Virus as a Possible Factor in Producing Dwarf Citrus Trees. *Fla. State Hort. Soc. Proc.* **1968**, 115–119.
48. Mendel, K. Interrelations between Tree Performance and Some Virus Diseases. In *International Organization of Citrus Virologists Conference Proceedings (1957–2010)*; IOCV: Riverside, CA, USA, 1968; Volume 4, pp. 310–313.
49. Bar-Joseph, M. Citrus Viroids and Citrus Dwarfing in Israel. In *Proceedings of the V International Symposium on Orchard and Plantation Systems 349*; 1992; pp. 271–276. Available online: https://www.actahort.org/books/349/349_45.htm (accessed on 29 March 2022).
50. Broadbent, P.; Forsyth, J.B.; Hutton, R.J.; Bevington, K.B. Guidelines for the Commercial Use of Graft-Transmissible Dwarfing in Australia—Potential Benefits and Risks. *Int. Citrus Congr.* **1992**, *7*, 697–701.

51. Schneider, H. The Anatomy of Citrus. In *The Citrus Industry II Anatomy, Physiology, Genetics and Reproduction*; Reuther, W., Batchelor, L.D., Webber, H.J., Eds.; University of California: Berkeley, CA, USA, 1968.
52. Burgess, A.L.; David, R.; Searle, I.R. Conservation of TRNA and RRNA 5-Methylcytosine in the Kingdom Plantae. *BMC Plant Biol.* **2015**, *15*, 199. [CrossRef] [PubMed]
53. Zimmermann, G.; Bäumlein, H.; Mock, H.-P.; Himmelbach, A.; Schweizer, P. The Multigene Family Encoding Germin-like Proteins of Barley. Regulation and Function in Basal Host Resistance. *Plant Physiol.* **2006**, *142*, 181–192. [CrossRef]
54. Wang, T.; Chen, X.; Zhu, F.; Li, H.; Li, L.; Yang, Q.; Chi, X.; Yu, S.; Liang, X. Characterization of Peanut Germin-like Proteins, AhGLPs in Plant Development and Defense. *PLoS ONE* **2013**, *8*, e61722. [CrossRef] [PubMed]
55. Xing, H.; Fu, X.; Yang, C.; Tang, X.; Guo, L.; Li, C.; Xu, C.; Luo, K. Genome-Wide Investigation of Pentatricopeptide Repeat Gene Family in Poplar and Their Expression Analysis in Response to Biotic and Abiotic Stresses. *Sci. Rep.* **2018**, *8*, 2817. [CrossRef]
56. Gidda, S.K.; Miersch, O.; Levitin, A.; Schmidt, J.; Wasternack, C.; Varin, L. Biochemical and Molecular Characterization of a Hydroxyjasmonate Sulfotransferase from Arabidopsis Thaliana. *J. Biol. Chem.* **2003**, *278*, 17895–17900. [CrossRef]
57. Simões, I.; Faro, C. Structure and Function of Plant Aspartic Proteinases. *Eur. J. Biochem.* **2004**, *271*, 2067–2075. [CrossRef]
58. Zhao, D.; Ni, W.; Feng, B.; Han, T.; Petrasek, M.G.; Ma, H. Members of the Arabidopsis-SKP1-like Gene Family Exhibit a Variety of Expression Patterns and May Play Diverse Roles in Arabidopsis. *Plant Physiol.* **2003**, *133*, 203–217. [CrossRef]
59. Helariutta, Y.; Fukaki, H.; Wysocka-Diller, J.; Nakajima, K.; Jung, J.; Sena, G.; Hauser, M.T.; Benfey, P.N. The SHORT-ROOT Gene Controls Radial Patterning of the Arabidopsis Root through Radial Signaling. *Cell* **2000**, *101*, 555–567. [CrossRef]
60. Dündar, E.; Bush, D.R. BAT1, a Bidirectional Amino Acid Transporter in Arabidopsis. *Planta* **2009**, *229*, 1047–1056. [CrossRef]
61. Hanaoka, H.; Noda, T.; Shirano, Y.; Kato, T.; Hayashi, H.; Shibata, D.; Tabata, S.; Ohsumi, Y. Leaf Senescence and Starvation-Induced Chlorosis Are Accelerated by the Disruption of an Arabidopsis Autophagy Gene. *Plant Physiol.* **2002**, *129*, 1181–1193. [CrossRef]
62. Wormit, A.; Usadel, B. The Multifaceted Role of Pectin Methylesterase Inhibitors (PMEIs). *Int. J. Mol. Sci.* **2018**, *19*, 2878. [CrossRef]
63. Lakehal, A.; Dob, A.; Rahneshan, Z.; Novák, O.; Escamez, S.; Alallaq, S.; Strnad, M.; Tuominen, H.; Bellini, C. Ethylene Response Factor 115 Integrates Jasmonate and Cytokinin Signaling Machineries to Repress Adventitious Rooting in Arabidopsis. *New Phytol.* **2020**, *228*, 1611–1626. [CrossRef]
64. Schubert, H.L.; Blumenthal, R.M.; Cheng, X. Many Paths to Methyltransfer: A Chronicle of Convergence. *Trends Biochem. Sci.* **2003**, *28*, 329–335. [CrossRef]
65. Fedotova, A.A.; Bonchuk, A.N.; Mogila, V.A.; Georgiev, P.G. C2H2 Zinc Finger Proteins: The Largest but Poorly Explored Family of Higher Eukaryotic Transcription Factors. *Acta Nat.* **2017**, *9*, 47–58. [CrossRef]
66. Li, N.; Liu, Z.; Wang, Z.; Ru, L.; Gonzalez, N.; Baekelandt, A.; Pauwels, L.; Goossens, A.; Xu, R.; Zhu, Z.; et al. STERILE APETALA Modulates the Stability of a Repressor Protein Complex to Control Organ Size in Arabidopsis Thaliana. *PLoS Genet.* **2018**, *14*, e1007218. [CrossRef]
67. Dinkins, R.; Pflipsen, C.; Thompson, A.; Collins, G.B. Ectopic Expression of an Arabidopsis Single Zinc Finger Gene in Tobacco Results in Dwarf Plants. *Plant Cell Physiol.* **2002**, *43*, 743–750. [CrossRef]
68. de Silva, K.; Laska, B.; Brown, C.; Sederoff, H.W.; Khodakovskaya, M. Arabidopsis Thaliana Calcium-Dependent Lipid-Binding Protein (AtCLB): A Novel Repressor of Abiotic Stress Response. *J. Exp. Bot.* **2011**, *62*, 2679–2689. [CrossRef]
69. Nagano, M.; Kakuta, C.; Fukao, Y.; Fujiwara, M.; Uchimiya, H.; Kawai-Yamada, M. Arabidopsis Bax Inhibitor-1 Interacts with Enzymes Related to Very-Long-Chain Fatty Acid Synthesis. *J. Plant Res.* **2019**, *132*, 131–143. [CrossRef]
70. Kruijt, M.; Brandwagt, B.F.; de Wit, P.J.G.M. Rearrangements in the Cf-9 Disease Resistance Gene Cluster of Wild Tomato Have Resulted in Three Genes that Mediate Avr9 Responsiveness. *Genetics* **2004**, *168*, 1655–1663. [CrossRef]
71. Patil, R.V.; Pawar, K.D. Comparative de Novo Flower Transcriptome Analysis of Polygamodioecious Tree Garcinia Indica. *3 Biotech* **2019**, *9*, 72. [CrossRef] [PubMed]
72. Abdullah-Zawawi, M.-R.; Ahmad-Nizammuddin, N.-F.; Govender, N.; Harun, S.; Mohd-Assaad, N.; Mohamed-Hussein, Z.-A. Comparative Genome-Wide Analysis of WRKY, MADS-Box and MYB Transcription Factor Families in Arabidopsis and Rice. *Sci. Rep.* **2021**, *11*, 19678. [CrossRef] [PubMed]
73. Ellinger, D.; Stingl, N.; Kubigsteltig, I.I.; Bals, T.; Juenger, M.; Pollmann, S.; Berger, S.; Schuenemann, D.; Mueller, M.J. Dongle and Defective in Anther Dehiscence1 Lipases Are Not Essential for Wound- and Pathogen-Induced Jasmonate Biosynthesis: Redundant Lipases Contribute to Jasmonate Formation. *Plant Physiol.* **2010**, *153*, 114–127. [CrossRef] [PubMed]
74. Boij, P.; Patel, R.; Garcia, C.; Jarvis, P.; Aronsson, H. In Vivo Studies on the Roles of Tic55-Related Proteins in Chloroplast Protein Import in Arabidopsis Thaliana. *Mol. Plant* **2009**, *2*, 1397–1409. [CrossRef] [PubMed]
75. Okuda, K.; Hammani, K.; Tanz, S.K.; Peng, L.; Fukao, Y.; Myouga, F.; Motohashi, R.; Shinozaki, K.; Small, I.; Shikanai, T. The Pentatricopeptide Repeat Protein OTP82 Is Required for RNA Editing of Plastid NdhB and NdhG Transcripts. *Plant J.* **2010**, *61*, 339–349. [CrossRef]
76. Kirik, V.; Kölle, K.; Wohlfarth, T.; Miséra, S.; Bäumlein, H. Ectopic Expression of a Novel MYB Gene Modifies the Architecture of the Arabidopsis Inflorescence. *Plant J.* **1998**, *13*, 729–742. [CrossRef]
77. Levy, M.; Wang, Q.; Kaspi, R.; Parrella, M.P.; Abel, S. Arabidopsis IQD1, a Novel Calmodulin-Binding Nuclear Protein, Stimulates Glucosinolate Accumulation and Plant Defense. *Plant J.* **2005**, *43*, 79–96. [CrossRef]

78. Bürstenbinder, K.; Savchenko, T.; Müller, J.; Adamson, A.W.; Stamm, G.; Kwong, R.; Zipp, B.J.; Dinesh, D.C.; Abel, S. Arabidopsis Calmodulin-Binding Protein IQ67-Domain 1 Localizes to Microtubules and Interacts with Kinesin Light Chain-Related Protein-1. *J. Biol. Chem.* **2013**, *288*, 1871–1882. [CrossRef]
79. Basu, D.; Tian, L.; Wang, W.; Bobbs, S.; Herock, H.; Travers, A.; Showalter, A.M. A Small Multigene Hydroxyproline-O-Galactosyltransferase Family Functions in Arabinogalactan-Protein Glycosylation, Growth and Development in Arabidopsis. *BMC Plant Biol.* **2015**, *15*, 295. [CrossRef]
80. Murgia, I.; Tarantino, D.; Soave, C.; Morandini, P. Arabidopsis CYP82C4 Expression Is Dependent on Fe Availability and Circadian Rhythm, and Correlates with Genes Involved in the Early Fe Deficiency Response. *J. Plant Physiol.* **2011**, *168*, 894–902. [CrossRef]
81. Léon-Kloosterziel, K.M.; Verhagen, B.W.M.; Keurentjes, J.J.B.; VanPelt, J.A.; Rep, M.; VanLoon, L.C.; Pieterse, C.M.J. Colonization of the Arabidopsis Rhizosphere by Fluorescent Pseudomonas Spp. Activates a Root-Specific, Ethylene-Responsive PR-5 Gene in the Vascular Bundle. *Plant Mol. Biol.* **2005**, *57*, 731–748. [CrossRef]
82. Che, P.; Lall, S.; Nettleton, D.; Howell, S.H. Gene Expression Programs during Shoot, Root, and Callus Development in Arabidopsis Tissue Culture. *Plant Physiol.* **2006**, *141*, 620–637. [CrossRef]
83. Nakano, T.; Suzuki, K.; Fujimura, T.; Shinshi, H. Genome-Wide Analysis of the ERF Gene Family in Arabidopsis and Rice. *Plant Physiol.* **2006**, *140*, 411–432. [CrossRef]
84. Diaz, M.; Sanchez-Barrena, M.J.; Gonzalez-Rubio, J.M.; Rodriguez, L.; Fernandez, D.; Antoni, R.; Yunta, C.; Belda-Palazon, B.; Gonzalez-Guzman, M.; Peirats-Llobet, M.; et al. Calcium-Dependent Oligomerization of CAR Proteins at Cell Membrane Modulates ABA Signaling. *Proc. Natl. Acad. Sci. USA* **2016**, *113*, E396–E405. [CrossRef]
85. Sharma, M.; Bhatt, D. The Circadian Clock and Defence Signalling in Plants. *Mol. Plant Pathol.* **2015**, *16*, 210–218. [CrossRef]
86. Roden, L.C.; Ingle, R.A. Lights, Rhythms, Infection: The Role of Light and the Circadian Clock in Determining the Outcome of Plant-Pathogen Interactions. *Plant Cell* **2009**, *21*, 2546–2552. [CrossRef]
87. Tauzin, A.S.; Giardina, T. Sucrose and Invertases, a Part of the Plant Defense Response to the Biotic Stresses. *Front. Plant Sci.* **2014**, *5*, 293. [CrossRef]
88. Gutierrez, C.K.; Matsui, G.Y.; Lincoln, D.E.; Lovell, C.R. Production of the Phytohormone Indole-3-Acetic Acid by Estuarine Species of the Genus Vibrio. *Appl. Environ. Microbiol.* **2009**, *75*, 2253–2258. [CrossRef]
89. Krueger, R.R.; Vidalakis, G. Study and Detection of Citrus Viroids in Woody Hosts. *Methods Mol. Biol.* **2022**, *2316*, 3–21. [CrossRef] [PubMed]
90. Vidalakis, G.; Gumpf, D.J.; Bash, J.A.; Semancik, J.S. Finger Imprint of Poncirus Trifoliata: A Specific Interaction of a Viroid, a Host, and Irrigation. *Plant Dis.* **2004**, *88*, 709–713. [CrossRef] [PubMed]
91. Vernière, C.; Perrier, X.; Dubois, C.; Dubois, A.; Botella, L.; Chabrier, C.; Bové, J.M.; Vila, N.D. Interactions between Citrus Viroids Affect Symptom Expression and Field Performance of Clementine Trees Grafted on Trifoliate Orange. *Phytopathology* **2006**, *96*, 356–368. [CrossRef] [PubMed]
92. Murcia, N.; Bernad, L.; Serra, P.; Hashemian, S.M.B.; Duran-Vila, N. Molecular and Biological Characterization of Natural Variants of Citrus Dwarfing Viroid. *Arch. Virol.* **2009**, *154*, 1329–1334. [CrossRef]